Residual entropy of ordinary ice from multicanonical simulations

Bernd A. Berg,[1,2,3] Chizuru Muguruma,[4] and Yuko Okamoto[3]
[1]*Department of Physics, Florida State University, Tallahassee, Florida 32306-4350, USA*
[2]*School of Computational Science, Florida State University, Tallahassee, Florida 32306-4120, USA*
[3]*Department of Physics, Nagoya University, Nagoya, Aichi 464-8602, Japan*
[4]*Faculty of Liberal Arts, Chukyo University, Toyota, Aichi 470-0393, Japan*
(Received 16 September 2006; published 21 March 2007)

We introduce two simple models with nearest-neighbor interactions on three-dimensional hexagonal lattices. Each model allows one to calculate the residual entropy of ice I (ordinary ice) by means of multicanonical simulations. This gives the correction to the residual entropy derived by Pauling [J. Am. Chem. Soc. **57**, 2680 (1935)]. Our estimate is found to be within less than 0.1% of an analytical approximation by Nagle [J. Math. Phys. **7**, 1484 (1966)], which is an improvement of Pauling's result. We pose it as a challenge to experimentalists to improve on the accuracy of a 1936 measurement by Giauque and Stout [J. Am. Chem. Soc. **58**, 1144 (1936)] by about one order of magnitude, which would allow one to identify corrections to Pauling's value unambiguously. It is straightforward to transfer our methods to other crystal systems.

DOI: 10.1103/PhysRevB.75.092202 PACS number(s): 61.50.Lt, 05.70.−a, 65.40.Gr

A thorough understanding of the properties of water has a long history and is of central importance for life sciences. After the discovery of the hydrogen bond,[1] it was recognized that the unusual properties of water and ice owe their existence to a combination of strong directional polar interactions and a network of specifically arranged hydrogen bonds.[2] The liquid phase of water differs from simple fluids in that there is a large qualitative remnant of ice structure in the form of local tetrahedral ordering.[3]

In contrast to liquid water, the properties of ice are relatively well understood. Most of them have been interpreted in terms of crystal structures, the forces between its constituent molecules, and the energy levels of the molecules themselves.[4,5] A two-dimensional projection of the hexagonal crystal structure of ordinary ice (ice I) is depicted in Fig. 1 (other forms of ice occur, in particular, at high pressures). Each oxygen atom is located at the center of a tetrahedron and straight lines (bonds) through the sites of the tetrahedron point toward four nearest-neighbor oxygen atoms. Hydrogen atoms are distributed according to the ice rules:[2,6] (A) There is one hydrogen atom on each bond (then called hydrogen bond). (B) There are two hydrogen atoms near each oxygen atom (these three atoms constitute a water molecule).

In our figure, distances are given in units of a lattice constant a, which is chosen to be the edge length of the tetrahedra (this is not the conventional crystallographic definition). For each molecule shown, one of the surface triangles of its tetrahedron is placed in the xy plane. The molecules labeled by u (up) are then at $z=1/\sqrt{24}$ above and the molecules labeled by d (down) at $z=-1/\sqrt{24}$ below the xy plane at the centers of their tetrahedra. In our computer simulations, information about the molecules will be stored in arrays of length N, N being the number of molecules.

Essentially by experimental discovery, extrapolating low-temperature calorimetric data (then available down to about 10 K) toward zero absolute temperature, it was found that ice has a residual entropy,[7]

$$S_0 = k \ln(W) > 0, \tag{1}$$

where W is the number of configurations for N molecules. Subsequently, Pauling[6] derived estimates of $W=(W_1)^N$ by two approximate methods, obtaining

$$W_1^{\text{Pauling}} = 3/2 \tag{2}$$

in each case. $W=(W_1)^N$ is the number of Pauling configurations. Assuming that the H_2O molecules are essentially intact in ice, his arguments are as follows.

(1) A given molecule can orient itself in six ways, satisfying ice rule B. Choosing the orientations of all molecules at random, the chance that the adjacent molecules permit a given orientation of the two hydrogen atoms is 1/4. The total number of configurations is thus $W=(6/4)^N$.

(2) Ignoring condition B of the ice rules, Pauling allows 2^{2N} configuration on the hydrogen bonds between adjacent oxygen atoms: Each hydrogen nucleus is given the choice of

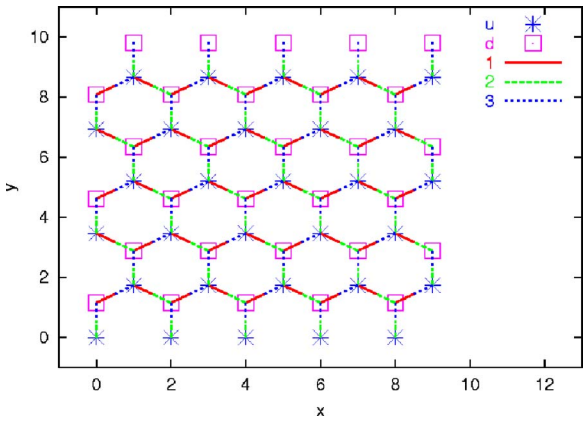

FIG. 1. (Color online) Lattice structure of one layer of ice I. The up (u) sites are at $z=1/\sqrt{24}$ and the down (d) sites at $z=-1/\sqrt{24}$. For each site, three of its four pointers to nearest-neighbor sites are shown.

two positions, near to one of the two oxygen atoms. At one oxygen atom, there are now 16 arrangements of the four hydrogen nuclei. Of those, ten are ruled out by ice rule B. For each oxygen atom this condition permits $6/16=3/8$ of the configurations. Accordingly, the total number of configurations becomes $W=2^{2N}(3/8)^N$.

Equation (2) converts to the residual entropy,

$$S_0^{\text{Pauling}} = 0.805\,74\cdots \text{ cal/deg mole}, \tag{3}$$

where we have used $R=8.314\,472(15)$ J/deg mol for the gas constant as of 20 August 2006 given on the NIST website[8] (relying on CODATA 2002 recommended values). This is in good agreement with the experimental estimate,

$$S_0^{\text{experimental}} = 0.82(5) \text{ cal/deg mole}, \tag{4}$$

which was subsequently obtained by Giauque and Stout[9] using refined calorimetry [we give error bars with respect to the last digit(s) in parentheses].

Pauling's arguments omit correlations induced by closed loops when one requires fulfillment of the ice rules for all atoms, and it was shown by Onsager and Dupuis[10] that $W_1=1.5$ is in fact a lower bound. Onsager's student Nagle used a series expansion method to derive the estimate,[11]

$$W_1^{\text{Nagle}} = 1.506\,85(15) \tag{5}$$

or

$$S_0^{\text{Nagle}} = 0.814\,80(20) \text{ cal/deg mole}. \tag{6}$$

Here, the error bar is not statistical but reflects higher-order corrections of the expansion, which are not entirely under control. The slight difference between Eq. (6) and the value in Nagle's paper is likely due to improvements in the measurements of Avogadro's number.[8] The only independent theoretical value appears to be one for cubic ice, which is obtained by numerical integration of Monte Carlo data[12] and is in good agreement with Nagle.[11]

Despite Nagle's high precision estimate, there has apparently been almost no improvement on the accuracy of the experimental value [Eq. (4)]. Some of the difficulties are addressed in a careful study by Haida *et al.*,[13] but their final estimate remains [Eq. (4)] with no reduction of the error bar. We noted that by treating the contributions in their Table 3 as statistically independent quantities and using Gaussian error propagation (instead of adding up the individual error bars), the final error bar becomes reduced by almost a factor of 2 and their value would then read $S_0=0.815(26)$ cal/deg mol. Still, Pauling's value is safely within one standard deviation. Modern electronic equipment should allow for a much better precision. We think that an experimental verification of the difference to Pauling's estimate would be an outstanding confirmation of structures imposed by the ice rules.

In this Brief Report we provide a high-precision numerical estimate of S_0 for ordinary ice. Our calculations are based on two simple statistical models, which reflect Pauling's arguments. Each model is defined on the hexagonal lattice structure of Fig. 1.

In the first model, called six-state H_2O molecule model, we allow for six distinct orientations of each H_2O molecule and define its energy by

$$E = -\sum_b h(b,s_b^1,s_b^2). \tag{7}$$

Here, the sum is over all bonds b of the lattice and (s_b^1 and s_b^2 indicate the dependence on the states of the two H_2O molecules, which are connected by the bond)

$$h(b,s_b^1,s_b^2) = \begin{cases} 1 & \text{for hydrogen bond} \\ 0 & \text{otherwise}. \end{cases} \tag{8}$$

In the second model, called two-state H-bond model, we do not consider distinct orientations of the molecule but allow two positions for each hydrogen nucleus on the bonds. The energy is defined by

$$E = -\sum_s f(s,b_s^1,b_s^2,b_s^3,b_s^4), \tag{9}$$

where the sum is over all sites (oxygen atoms) of the lattice. The function f is given by

$$f(s,b_s^1,b_s^2,b_s^3,b_s^4) = \begin{cases} 2 & \text{for two hydrogen nuclei close to } s \\ 1 & \text{for one or three hydrogen nuclei close to } s \\ 0 & \text{for zero or four hydrogen nuclei close to } s. \end{cases} \tag{10}$$

The ground states of each model fulfill the ice rules. At $\beta=0$, the number of configurations is 6^N for the six-state model and 2^{2N} for the two-state model. Because the normalizations at $\beta=0$ are known, multicanonical (MUCA) simulations[14] allow us in either case to estimate accurately the number of ground-state configurations.[15] Superficially, both systems resemble Potts models (see, e.g., Ref. 16 for Potts model simulations), but their thermodynamic properties are entirely different. For instance, we do not find any sign of a disorder-order phase transition, which is for our purposes advantageous as the MUCA estimates for the ground-state entropy become particularly accurate. This absence of a bulk transition does not rule out long-range correlations between bonds of the ground-state configurations, which are imposed by the conservation of the flow of hydrogen bonds at each molecule. In that sense, the ground state is a critical ensemble.

Using periodic boundary conditions (BCs), our simulations are based on a lattice construction set up earlier by one of us.[17] Following closely the method outlined in Chapter 3.1.1 of Ref. 16 four index pointers from each molecule to the array positions of its nearest-neighbor molecules are constructed. The order of pointers one to three is indicated in Fig. 1. The fourth pointer is up the z direction for the u molecules and down the z direction for the d molecules. The lattice then contains $N=n_x n_y n_z$ molecules, where n_x, n_y, and n_z are the number of sites along the x, y, and z axes, respectively. The periodic BCs restrict the allowed values of n_x, n_y, and n_z to $n_x=1,2,3,\ldots$, $n_y=4$, 8, 12,..., and $n_z=2$, 4, 6,.... Otherwise, the geometry does not close properly. Using the

TABLE I. Simulation data for W_1.

				Six-state model		Two-state model		
N	n_x	n_y	n_z	W_1	N_{cyc}	W_1	N_{cyc}	Q
128	4	8	4	1.52852 (47)	1854	1.52869 (23)	7092	0.72
360	5	12	6	1.51522 (49)	223	1.51546 (15)	1096	0.65
576	6	12	8	1.51264 (18)	503	1.51279 (10)	1530	0.47
896	7	16	8	1.51075 (16)	208	1.51092 (06)	2317	0.32
1600	8	20	10	1.50939 (09)	215	1.50945 (05)	619	0.56
	∞ (fit)			1.50741 (33)		1.50737 (17)		0.91

intersite distance $r_{\mathrm{OO}}=2.764$ Å from Ref. 5, the physical size of the box is obtained by putting the lattice constant a to $a=2.257$ Å, and the physical dimensions of the box are calculated to be $B_x=2n_xa$, $B_y=(n_y\sqrt{3}/2)a$, and $B_z=(n_z4/\sqrt{6})a$. In our choices of n_x, n_y, and n_z values, we aimed within reasonable limitations at symmetrically sized boxes.

Table I compiles our MUCA W_1 estimates for the lattice sizes used. In each case, a Wang-Landau recursion[18] was used to estimate the MUCA parameters, for which, besides a certain number of cycling events,[16] a flatness of $H_{\mathrm{min}}/H_{\mathrm{max}}>0.5$ was considered sufficient to stop the recursion and start the second part of the MUCA simulation with fixed weights [$H(E)$ is the energy histogram, H_{min} is the smallest, and H_{max} is the largest number of entries in the flattened energy range].

The statistics we used for measurements varied between 32×10^6 sweeps for our smallest and 64×10^7 sweeps for our largest lattice. By using two 2 GHz personal computers (PCs), the simulations take less than one week. The number of cycles N_{cyc} completed between $\beta_{\mathrm{min}}=0$ and the ground state are listed in the six-state and two-state model columns of Table I. As each of our simulations includes the $\beta_{\mathrm{min}}=0$ canonical ensemble, the (logarithmically coded) reweighting procedure of Chapter 5.1.5 of Ref. 16 delivers estimates for W_1, which are compiled in the same columns. Each error bar relies on 32 jackknife bins. As expected, the values from both models are consistent, as demonstrated by Q values of Gaussian difference tests (see, e.g., Chapter 2.1.3 of Ref. 16) in the last column of the table. The two-state H-bond model gives more accurate estimates than the six-state H_2O molecule model, obviously by the reason that the cycling time, which is $\propto 1/N_{\mathrm{cyc}}$, is less for the former because the energy range that needs to be covered is smaller.

In Fig. 2, a fit for the data of the two-state H-bond model to the form

$$W_1(x)=W_1(0)+a_1x^{\theta},\quad x=1/N \tag{11}$$

is shown. The $W_1=W_1(0)$ estimate from Fig. 2 is given in the last row of the two-state model column of Table I. The data point for the smallest lattice is included in the fit, but not shown in the figure where we want to focus on the large N region. The goodness of fit (Chapter 2.8 of Ref. 16) is $Q=0.47$, as given in the figure. Similarly, the estimate for the six-state H_2O molecule model in the last row of the table is obtained with a goodness of fit $Q=0.78$. All Q values (Gaussian difference tests and fits) are in the range one would expect for statistically consistent data. The θ values of the fits are also consistent and their combined value is $\theta=0.923(23)$. That we have $\theta\neq1$ reflects bond correlations in the ground-state ensemble.

Combining the two fit results weighted by their error bars leads to our final estimate,

$$W_1^{\mathrm{MUCA}}=1.507\,38(16). \tag{12}$$

This converts into

$$S_0^{\mathrm{MUCA}}=0.815\,50(21)\ \mathrm{cal/deg\ mole} \tag{13}$$

for the residual entropy.

The difference between Eq. (12) and the estimate of Nagle [Eq. (5)] is 0.035% of the estimated W_1 value (0.086% of S_0), which is much smaller than any foreseeable experimental error. However, within their own error bars, the Gaussian difference test between the two estimates yields $Q=0.016$. As the error bar in Eq. (12) covers only statistical errors and not systematic errors due to finite size corrections from larger lattices, the small discrepancy with Nagle's result may well be explained this way. In view of the large error bar in the experimental estimate, it appears somewhat academic to trace the ultimate reason.

As already (hesitatingly) pointed out by Pauling,[6] the real entropy at zero temperature is not expected to agree with the residual entropy extrapolated from low but nonzero tempera-

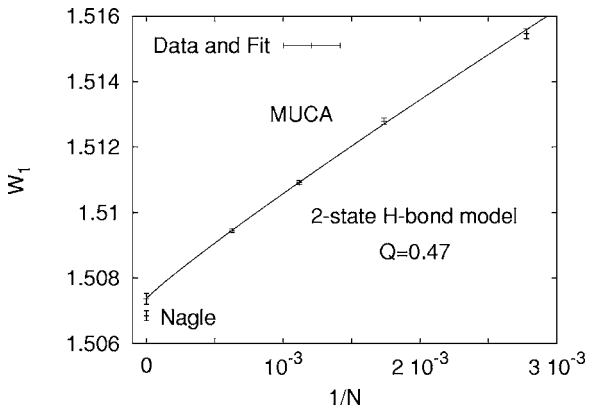

FIG. 2. Fit for W_1.

tures. In real ice, one expects a small splitting of the energy levels of the Pauling configuration, which are degenerate in both of our models. Once the thermal fluctuations become small compared with these energy differences, the entropy will become lower than the residual entropy calculated here. Such an effect is observed in Ref. 13 by annealing ice I at temperatures between 85 and 110 K. Refined models are needed to gain computational insights. Crossing this temperature range sufficiently fast still allows one to extract the present residual entropy, because the relaxation time has become so long that one does not have ordering of Pauling states during typical experimental observation times.

It is clear that our method rather easily carries over to other crystal structures for which one may want to calculate residual entropies. In particular, structural defects and impurities can be included, although one may have to use more realistic energy functions, and lattice sizes to put limits on low densities. Simulations very similar to those performed here should enable accurate estimates of the residual entropies for other forms of ice and various geometrically frustrated systems[19] as well as for spin models in the class for which lower bounds on their residual entropies were derived in. Ref. 20. For more involved systems, our approach is to design simple models, which share the relevant ground-state symmetries with the system of interest. That could, for instance, have applications to the residual entropy of proteins by allowing for more realistic modeling than that done in Ref. 21.

Finally, good modeling of water is of crucial importance for computational progress in biophysics. Clusters of hydrogen bonds play a prominent role in water at room temperature. Our method allows one to calculate the combinatorial factors W_1^N with which small clusters ought to be calculated in phenomenological water models like those discussed in Ref. 3. Through a better understanding of hydrogen bond clusters, insights derived from the study of ordinary ice may well be of importance for improving on models,[22] which have primarily been constructed to reflect properties of water under room temperatures and pressures.

We like to thank John Nagle for email comments on the first version of this paper. During most of this work, B.A.B. was supported by the JSPS. C.M. and Y.O. were supported, in part, by the Ministry of Education, Culture, Sports, Science and Technology (MEXT), Japan: C.M. by Grants-in-Aid for Young Scientists (B), Grant No. 16740244 and Y.O. by Grants-in-Aid for the Next Generation Super Computing Project, Nanoscience Program and for Scientific Research in Priority Areas, Water and Biomolecules.

[1] W. M. Latimer and W. H. Rodebush, J. Am. Chem. Soc. **42**, 1419 (1920).
[2] J. D. Bernal and R. H. Fowler, J. Chem. Phys. **1**, 515 (1933).
[3] H. S. Frank and W.-Y. Wen, Discuss. Faraday Soc. **24**, 133 (1957); G. Némethy and H. A. Scheraga, J. Chem. Phys. **36**, 3382 (1962); F. Sciortino, A. Geiger, and H. E. Stanley, *ibid.* **96**, 3857 (1992).
[4] D. Eisenberg and W. Kauzmann, *The Structure and Properties of Water* (Oxford University Press, Oxford, 1969).
[5] V. F. Petrenko and R. W. Whitworth, *Physics of Ice* (Oxford University Press, Oxford, 1999).
[6] L. Pauling, J. Am. Chem. Soc. **57**, 2680 (1935).
[7] W. F. Giauque and M. Ashley, Phys. Rev. **43**, 81 (1933).
[8] National Institute of Standards and Technology (NIST), http://physics.nist.gov/cuu/
[9] W. F. Giauque and J. W. Stout, J. Am. Chem. Soc. **58**, 1144 (1936).
[10] L. Onsager and M. Dupuis, Rend. Sc. Int. Fis. "Enrico Fermi" **10**, 294 (1960).
[11] J. F. Nagle, J. Math. Phys. **7**, 1484 (1966).
[12] S. V. Isakov, K. S. Raman, R. Moessner, and S. L. Sondhi, Phys. Rev. B **70**, 104418 (2004).
[13] O. Haida, T. Matsuo, H. Suga, and S. Seki, J. Chem. Thermodyn. **6**, 815 (1974).
[14] B. A. Berg and T. Neuhaus, Phys. Rev. Lett. **68**, 9 (1992).
[15] B. A. Berg and T. Celik, Phys. Rev. Lett. **69**, 2292 (1992).
[16] B. A. Berg, *Markov Chain Monte Carlo Simulations and Their Statistical Analysis* (World Scientific, Singapore, 2004).
[17] B. A. Berg (unpublished).
[18] F. Wang and D. P. Landau, Phys. Rev. Lett. **86**, 2050 (2001).
[19] R. Higashinakawa, H. Fukazawa, K. Degushi, and Y. Maeno, J. Phys. Soc. Jpn. **73**, 2845 (2004) and references therein.
[20] Y. Chow and F. Y. Wu, Phys. Rev. B **36**, 285 (1987).
[21] Z. Li, S. Raychaudhuri, and A. J. Wand, Protein Sci. **5**, 2647 (1996).
[22] See references collected in C. Vega, E. Sanz, and J. L. F. Abascal, J. Chem. Phys. **122**, 114507 (2005).